CEBAF PROPOSAL COVER SHEET

This Proposal must be mailed to:

CEBAF
Scientific Director's Office
12000 Jefferson Avenue
Newport News, VA 23606

and received on or before 1 October 1991.

A. TITLE:

Search for "Missing Resonances in the Electroproduction of Omega Mesons

B. CONTACT PERSON:

Herbert Funsten

ADDRESS, PHONE, AND ELECTRONIC MAIL ADDRESS:

College of William & Mary, Department of Physics
Williamsburg, Va 23185
(804) 221-3515
Funsten @ CEBAF

C. IS THIS PROPOSAL BASED ON A PREVIOUSLY SUBMITTED PROPOSAL OR LETTER OF INTENT?

[ ] YES [X] NO

IF YES, TITLE OF PREVIOUSLY SUBMITTED PROPOSAL OR LETTER OF INTENT:

****

(CEBAF USE ONLY)

Receipt Date 1 Oct 91

Log Number Assigned PR-91-024

By [redacted]

Search for "Missing" Resonances in the Electroproduction of ω Mesons

Spokespersons: V. Burkert, H. Funsten, and M. Manley

The N^* Group in the CLAS Collaboration

V. Burkert, D. Joyce, B. Mecking, M. Mestayer, B. Niczyporuk,
E. Smith, A. Yegneswaran
CEBAF, Newport News, Virginia

D. Crabb, D. Day, R. Marshall, J. McCarthy, R. Minehart
O. Rondon-Aramayo, R. Sealock, L.C. Smith, S. Thornton, H.J. Weber
University of Virginia, Charlottesville, Virginia

P. Stoler, G. Adams, N. Mukhopadyay
Rensselaer Polytechnic Institute, Troy, New York

K. Beard, C. Carlson, H. Funsten
College of William and Mary, Williamsburg, Virginia

D. Isenhower, M. Sadler
Abilene Christian University, Abilene, Texas

D. Doughty, D. Heddle
Christopher Newport College, Newport News, Virginia

L. Dennis, A. Tam
Florida State University, Tallahassee, Florida

S. Dytman, T. Donoghue
University of Pittsburg, Pittsburg, Pennsylvania

J. Lieb
George Mason University, Fairfax, Virginia

K. Giovanetti
James Madison University, Harrisonburg, Virginia

M. Manley
Kent State University, Kent, Ohio

C. Stronach
Virginia State University, Petersburg, Virginia

M. Gai
Yale University, New Haven, Connecticut

Abstract

Electroproduction of ω mesons (ep $\rightarrow$ e'pω) will be used to search for a group of "missing" N* resonances in the mass region between threshold and 2.2 GeV. These resonances have been predicted by quark models but have not yet been experimentally confirmed. Using the CEBAF Large Acceptance Spectrometer CLAS, the recoiling proton will be detected in coincidence with the scattered electron. In addition, the $\pi^-\pi^+$ pair from the ω decay can be detected. This will not only improve the signal/noise ratio but also make it possible to perform an analysis of the ω polarization. The cross section for the production of ω in the backward direction and the ω polarization are expected to be especially sensitive to resonance contributions.

A. Introduction

The non-relativistic quark model with QCD-inspired improvements has been very successful in describing the properties of the known baryons. However, the predicted number of excited baryon states (resonances) is considerably larger than the number of states that have been observed experimentally. Failure to find these resonances would create a serious problem for the non-relativistic quark model and indicate that the basic degrees of freedom in 3 quark systems are not well understood. For example, it has been conjectured that the quark degrees of freedom are restricted to oscillations of a quark-diquark system.

An explanation which doesn't invoke restricting the quark degrees of freedom has been developed [1]. It explains the lack of observation of these "missing" resonances as an experimental problem. Most N* resonances have been observed in pion scattering experiments. This permitted only the observation of those resonances that have an appreciable πN coupling. Particularly, in the case of elastic πN scattering via a resonance, the cross section is proportional to the fourth power of the πN coupling. Weak πN coupling results in the resonance being masked by neighboring resonances with stronger πN coupling. Koniuk and Isgur [1] have shown that many unobserved resonances indeed decouple from the πN channel. Their small πN coupling is caused by color hyperfine splitting between the constituent quarks producing configuration mixing both within and between SU(6) multiplets. Other decay channels such as γN, ωN, ρN, and $\pi\Delta$ are not affected by this mixing, and the "missing" resonances retain a total width characteristic of other known resonances. Hence, the only practical way to observe "missing" resonance formation is via (γN $\rightarrow$ ωN, ρN, or $\pi\Delta$) reactions.

The ωN decay channel is well suited to search for "missing" resonances because of the relative narrow ω meson decay width (Γ_ω =8.5 MeV), compared

to the ρ meson (Γ_ρ = 153 MeV). The hadronic final state can be identified in e p$\rightarrow$ e'p X using missing mass techniques. The ωN channel should be very sensitive to "missing" resonances because:

a) the isoscalar ω meson can couple with the proton only to $N^*(I = 1/2)$ resonances. There are no $\Delta(I = 3/2)$ resonance contributions to ωp final states.

b) the decays of the known N* resonances proceed predominantly via Nπ, $\Delta\pi$, Nρ, and Nη final states. There are no N* known that have a measurable ω decay branch [4]. (There are several resonances, e.g. the $P_{11}(1700)$ and $P_{13}(1700)$, whose total inelasticity is not fully accounted for by the known decay modes. These resonances could enhance ω production near threshold, similar to the Roper resonance enhancement in the $I = 1/2$ component of the $\pi N \rightarrow \pi\pi N$ reaction).

Quark model predictions by Koniuk [5] and Isgur [3] show that the ωN decay of "missing" N* resonances is generally as strong as the other non-(πN) decays. They list eight low-lying N* states (states for which the orbital angular momentum ≤ 2 and radial excitation number ≤ 1) that have not been observed. Table I [3] lists these together with two Δ resonances. All ωN couplings are considerably larger than the πN couplings.

The Feynman diagrams for the processes contributing to ω production are shown in Fig. 1. The two non-resonant processes, $t-$channel π exchange and diffraction are strong and could easily mask a resonance signal. In π exchange, ω production occurs via π^0 exchange with the incident photon. The amplitude for this process is significant due to the relatively large (8%) $\omega \rightarrow \pi^0\gamma$ branch. In diffractive production, the incident photon turns into a virtual ω (Vector Meson Dominance, VMD) and then diffractively scatters off the proton. Both processes have large cross sections at small momentum transfers, corresponding to forward angles. Therefore, a search for the contribution of resonances to ω production has to concentrate on backward angles.

B. Existing Data

Differential cross section data for backward ω electroproduction in the resonance region are sparse as can be seen in Figs. 2 and 3, [8,9]. No attempt has been made in the previous work to study the variation of backward cross section with W. In the work by Ballam et al. (W = 2.5 GeV), shown in Fig. 3, no results were reported for the backward region. In the ω electroproduction data by Joos et al., Fig 2., (W = 1.7 - 2.0 GeV), there is evidence for a leveling off of the differential cross section at backward angles. Joos notes that his data cannot be explained by π exchange and diffraction alone and suggests that:

"formation of s-channel resonances contributes
strongly in ω electroproduction for W $\leq$ 2 GeV"

The same flattening out appears in the photoproduction data of the ABBHHM collaboration (W = 1.8 - 2.0 GeV), Figs. 2 and 3. The two ABBHHM data points (solid boxes) at back angles are considerably above the calculated non-resonant cross section produced by diffraction and π exchange, (solid curve of Fig. 3, see section C for details). The surprisingly large backward cross section is, however, consistent with the formation of a "missing" resonance with the expected γ and ω couplings (dashed curve of Fig. 3).

C. Cross Section Calculation

Calculations were performed to determine the sensitivity of ω production cross sections and ω decay correlation measurements to the existence of the group of "missing" resonances. As a prototype, the $N^{\star\frac{5}{2}}(1955)$ member of the group was selected for the calculation because of its predicted features [3,5]:

- it has a strong photon coupling, nearly one third of the $\Delta(1232)$ photon coupling

- it has the strongest ω coupling in the "missing" resonance group

- it has an almost vanishing πN coupling, only 1/30 the ωN coupling (difficult to detect in pion induced formation)

- its relatively high spin, J = 5/2, characteristic of many resonances in the group, will generate a high multipole angular distribution in the resonance center-of-mass system (cms). This should facilitate the separation of the resonance from the background.

a) Differential Cross Sections

The differential cross section for ω production resulting from the three contributions (s - channel resonance, VMD diffractive, and t - channel π exchange, see Fig. 1) was calculated by adding the resonance amplitude to the π exchange and diffractive amplitudes as given in [6]. A centrifugal ω barrier penetration factor of the form $(q_\omega(W)/q_\omega(W{=}1955))^{3/2}$ was used where q_ω is the ω momentum in the cms. The $N^{\star\frac{5}{2}}(1955)$ resonance helicity amplitudes, taken from [3] and [5], are typical for the group of "missing" resonances in the $1.8 \leq W \leq 2.1$ GeV region. The two non-resonant processes dominate the forward direction; the ratio of non-resonant forward/backward ω production in the cms system is $\approx$ 200/1. Figure 3 shows the differential cross section at W = 1955 MeV as a function of θ^*_ω (the ω angle in the cms) with and without the $N^{\star\frac{5}{2}}(1955)$ resonance. The photon and ω coupling constants were taken from Table I. The backward ω production is dominated by the $N^{\star\frac{5}{2}}(1955)$ resonance formation.

Figure 9 shows the differential cross section at $\theta^*_\omega = 180°$ as a function of W yielding the typical "bump" at the resonance energy.

b) ω Decay Correlation

Detecting the $\pi^-\pi^+$ pair from the $\omega \to \pi^-\pi^+\pi^0$ decay in coincidence with the proton will allow the complete kinematical reconstruction of the reaction $\gamma_v p \to \omega p \to \pi^-\pi^+\pi^0 p$ and the determination of the decay plane of the ω, yielding additional sensitivity to resonance formation. The decay correlation, $W(\theta_{decay}, \phi_{decay})$, describes the variation of the ω production cross section with the orientation of the $\omega \to \pi^-\pi^+\pi^0$ decay plane. The orientation of the plane is described by the direction of the normal to the $\pi^-\pi^+\pi^0$ decay plane in the cms of the decaying ω. The angles θ_{decay} and ϕ_{decay} are defined relative to the outgoing proton (z axis) and the reaction plane (x axis). The ω density matrix elements from the differential cross section calculation were used in the decay correlation expression of [11] to determine $W(\theta_{decay}, \phi_{decay})$. Figures 10 and 11 show $W(\theta_{decay}, \phi_{decay})$ evaluated at W = 1955 MeV and $\theta^* = 180°$ with and without the prototype resonance. Due to interference between the three contributing processes that populate different ω helicity states, there is clear sensitivity to resonance formation in the correlation pattern.

D. Experimental Procedure

The proposed experiment will use the CEBAF Large Acceptance Spectrometer to measure ω electroproduction off the proton. The main goal of the experiment is to measure differential cross section for ω production as a function of the the mass of the hadronic system W (from threshold to $\approx$ 2.2 GeV) and the ω production angle θ^*_ω. Differential cross sections will be measured, detecting the recoiling proton in coincidence with the scattered electron ($ep \to e'pX$) and using the missing mass technique to identify the unobserved ω. A subset of the data will contain $\pi^-\pi^+$ pairs from the ω decay. This allows to

a) improve the signal/noise ratio, likely to be important in the backward direction where cross sections are known to be small

b) determine the decay angle correlation which is especially sensitive to resonance production.

Ideally, the data acquisition system should be triggered by the detection of a scattered electron, thus giving an unbiased data sample for the hadronic final state.

E. Simulation of the Experiment

Monte Carlo techniques were used to generate events from the ($ep \to e'pX$) reaction and to study the response of the CLAS detector. All relevant reaction channels were included. CLAS resolution and acceptance were taken into

account to derive the missing mass resolution, the signal/noise ratio for ω detection, and the acceptance as a function of the ω cms angle.

Figure 4 shows the results of the simulation for the missing mass distribution $(m_X)^2$ derived from detecting only the scattered electron and the proton $(ep \rightarrow e'pX)$. The $(m_X)^2$ distribution contains an ω peak at 0.61 GeV^2 on top of a continuum of mostly two-pion final states resulting from ρ and $\Delta\pi$ production. In addition, there is a small contribution of 3π final states that do not result from ω decays.

By requiring the detection of a $\pi^-\pi^+$ pair in coincidence most of this continuum background can be eliminated. Figure 5 shows the result of the simulation for the mass squared distribution, $(m_{\pi^-\pi^+})^2$, for all $\pi^-\pi^+$ pairs from the final states mentioned above. Due to the missing π^0 in the ω decay there is little overlap between the $(m_{\pi^-\pi^+})^2$ distribution generated by ω and ρ decay. Applying a cut on the $(m_{\pi^-\pi^+})^2$ distribution eliminates the two-pion background underneath the ω peak in the $(m_X)^2$ distribution completely. Figure 6 shows the $(m_X)^2$ distribution with the cut on $(m_{\pi^-\pi^+})^2$. The remaining background under the ω peak arises from 3 pion final states. The broad distribution below 0.4 GeV^2 is mainly due to $\Delta\pi \rightarrow p\pi^-\pi^+$ final states.

The detection efficiency for the $(ep \rightarrow e'p\omega)$ reaction was determined as a function of θ^*_ω taking the kinematics of the reaction and the acceptance of CLAS into account. Figure 7 shows the efficiency for detecting the recoiling proton only, Fig. 8 gives the efficiency for the coincident detection of the $p\pi^-\pi^+$ final state. (The efficiency figures do not include the limited azimuthal acceptance for the scattered electron; this will reduce count rates by a factor of 2). The efficiency variation with θ^*_ω is mainly caused by the azimuthal acceptance of CLAS that decreases for forward going particles. Note that the full θ^*_ω range can be covered. has

F. Count Rate Estimates

The following assumptions were used in estimating the ω count rate due to resonance formation:

Electron beam energy: $E_0 = 4$GeV

Luminosity: L $= 10^{34} cm^{-2} \cdot sec^{-1}$

Virtual photon flux /incident electron / $(\Delta W \cdot \Delta Q^2) = 1.8 \cdot 10^{-3} GeV^{-3}$. The flux, evaluated at W = 2.0 GeV, is an average over $0.5 \leq Q^2 \leq 0.8 GeV^2$, $(14^\circ \leq \theta_e \leq 19^\circ)$.

Total ω production cross section due to $N^{*\frac{5}{2}}(1955)$ formation: $\sigma_{total}(\gamma p \rightarrow N^* \rightarrow p\omega) = 1.0 \mu b$

CLAS average efficiency = 0.075 for detection of the e'p$\pi^-\pi^+$ final state particles. This was obtained from the CLAS simulation calculation described in Sec. E.

Size of Q^2 bin = 0.3 GeV^2.

Size of W bin = 0.05 GeV.

Size of θ^*_ω bin = 15°, number of bins = 12

The resulting count rate (due to resonance formation alone!) is 10^3 /week /θ^*_ω bin. The experiment will be able to obtain approximately 3% statistics per week per θ^*_ω bin at back angles.

Using the simulated 3π continuum background component under the ω peak, the proposed experiment can detect a resonance contribution of 13 nanobarns/sr in a θ^*_ω-bin per week running time.

Size of θ_{decay} bin = 18°, number of bins = 10

Size of ϕ_{decay} bin = 18°, number of bins = 10. (Note that W($\theta_{decay}, \phi_{decay}$) is symmetric about ϕ = 180°).

The ω decay angular correlation will give an additional signature for a resonance. The ω decay correlation count rate is 10/(θ^*_ω-bin)/(θ_{decay}-bin)/(ϕ_{decay}-bin) per week.

G. Run Time Request

The running conditions of this experiment are identical to the conditions of some of the experiments proposed by the N* Collaboration. A total of 500 hours of beam time (to be split between 2 and 4 GeV, and hydrogen and deuterium targets) has been approved for all N* Collaboration experiments. No additional run time will be requested at this time. Note, however, that only the run time with 4 GeV electrons on the hydrogen target will be useful for the "missing" resonance search.

H. Summary

The proposed experiment represents a first step in the search for a group of "missing" N* resonances in the mass region around 2 GeV. These resonances have been predicted by quark models but have not yet been experimentally confirmed. The experiment will investigate the ωN decay of these resonances. The backward ω production cross section and the orientation of the ω decay plane are expected to be especially sensitive to resonance contributions.

Using the CEBAF Large Acceptance Spectrometer CLAS, all charged particles in the final state can be detected in coincidence with reasonable detection efficiency.

Should the experiment find evidence for "missing" resonances in the ωN channel it is likely that more detailed investigations will be required to identify and disentangle the contributing resonances.

References

[1] R. Koniuk and N. Isgur, Phys. Rev. D 21, p. 1868 (1980)

[2] N. Isgur and G. Karl, Phys. Rev. D 19, p. 2653 (1979)

[3] N. Isgur, Proceedings of the CEBAF/SURA 1984 Summer Workshop, F. Gross and R.R. Whitney, Eds., p. 219

[4] J.J. Hernandez *et al.*, Review of Particle Properties, Particle Data Group, Phys. Lett. B239 (1990)

[5] R. Koniuk, Nucl. Phys. B195, p. 452 (1980). See also ref. 3.

[6] B. Fraas, Nucl. Phys. B36 p. 191 (1972)

[7] Bauer *et al.*, Rev. of Mod. Phys. Vol. 50, p. 327 (1978)

[8] J. Ballam *et al.*, Phys. Rev. D7, p. 2166

[9] P. Joos *et al.*, Nucl. Phys. B122, p. 365 (1977)

[10] ABBHHM Collaboration, Phys. Rev. 175 p. 1669 (1968).

[11] K. Schilling *et al.*, Nucl. Phys. B15, p. 397 (1970)

Figure Captions

Figure 1 Feynman diagrams for the three processes taken into account for the calculation of the electromagnetic production of ω mesons.

Figure 2 Differential cross section for ω photo- (open circles) and electro- (black circles) production, reproduced from Fig. 5, Joos et al. [9].

Figure 3 Calculated differential cross section for ω electroproduction in the limit $Q^2 = 0$ at W = 1955 MeV. The large forward cross section is due to π exchange and diffraction scattering, in about equal amounts. The solid curve is without the resonance, the dashed line is with the resonance. Also plotted are ω photoproduction data of Ballam *et al.*, ref. 8, (open circles) taken at W = 2.5 GeV and scaled to W = 1.955 GeV.

Figure 4 Monte Carlo calculation for the missing mass squared $(m_X)^2$ in $(ep \rightarrow e'pX)$ showing peaks due to π^0, η, and ω production. The broad bump underneath the ω is due to ρ production.

Figure 5 Monte Carlo calculation for the mass distribution of $\pi^-\pi^+$ pairs, $(m_{\pi^-\pi^+})^2$ showing the contributions from ρ and ω production.

Figure 6 Monte Carlo calculation for the missing mass distribution, $(m_X)^2$, in coincidence with $\pi^-\pi^+$ pairs. A cut was placed to accept pairs only below $(m_{\pi^-\pi^+})^2 = 0.42$ GeV^2. The broad peak underneath the ω peak arises from non-resonant 3 π final states.

Figure 7 Monte Carlo calculation for the CLAS detection efficiency for protons from ω electroproduction.

Figure 8 Monte Carlo calculation for the CLAS detection efficiency for the complete $p\pi^-\pi^+$ final state.

Figure 9 Result of a model calculation for the ω electroproduction differential cross section at $\theta^* = 180°$ versus W with and without the $N^{*\frac{1}{2}}$ resonance.

Figure 10 Result of a model calculation for the ω decay angular correlation, $W(\theta_{decay}, \phi_{decay})$, evaluated at W = 1955 MeV and $\theta^* = 180°$ for $\omega \rightarrow \pi^-\pi^+\pi^0$ decay in the presence of the $N^{*\frac{1}{2}}$ resonance. The angles θ_{decay} and ϕ_{decay} are defined in the text.

Figure 11 $W(\theta_{decay}, \phi_{decay})$ without the resonance contribution.

TABLE 1 : Some Missing Baryon Resonances (and Where to Find Them)

state	photoproduction amplitudes $A^p_{3/2}$	$A^p_{1/2}$	$A^n_{3/2}$	$A^n_{1/2}$	strong coupling amplitudes Nπ	Δπ	Nρ	Nω
$N\frac{5+}{2}(1955)$	+ 9	-67	-45	-22	0	- 7	- 8	+12
$N\frac{5+}{2}(2025)$	- 3	+ 2	+51	+15	1	- 7	+ 7	-11
$\Delta\frac{5+}{2}(1975)$	+76	+61			1	+ 6	-18	na
$N\frac{3+}{2}(1870)$	+ 6	-19	- 6	-21	3	- 4	+ 1	-10
$N\frac{3+}{2}(1955)$	+ 4	-16	-39	+ 6	1	- 9	+ 6	- 9
$N\frac{3+}{2}(1980)$	- 5	+19	+22	-20	1	+ 9	- 7	+ 3
$N\frac{3+}{2}(2060)$	0	- 1	-15	+ 2	1	+ 5	- 3	+ 9
$\Delta\frac{3+}{2}(1975)$	- 7	+18			0	- 8	+ 5	na
$N\frac{1+}{2}(1890)$		-20		- 1	4	+ 3	- 5	+ 6
$N\frac{1+}{2}(2055)$		+ 7		+ 3	1	+ 2	- 1	- 5

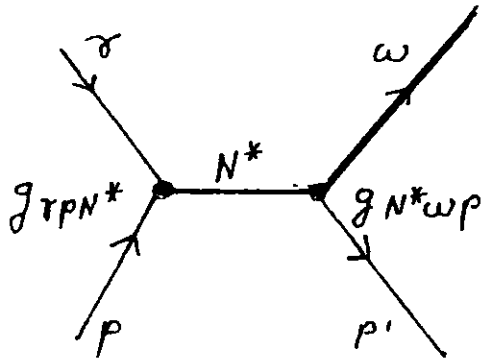

s-channel
resonance

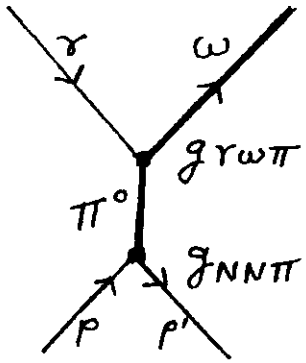

t-channel
π exchange

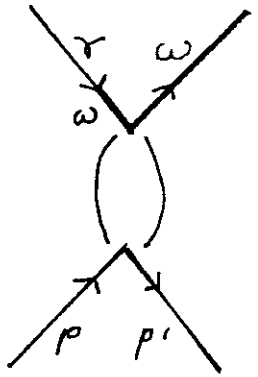

diffractive
scattering

Fig.1

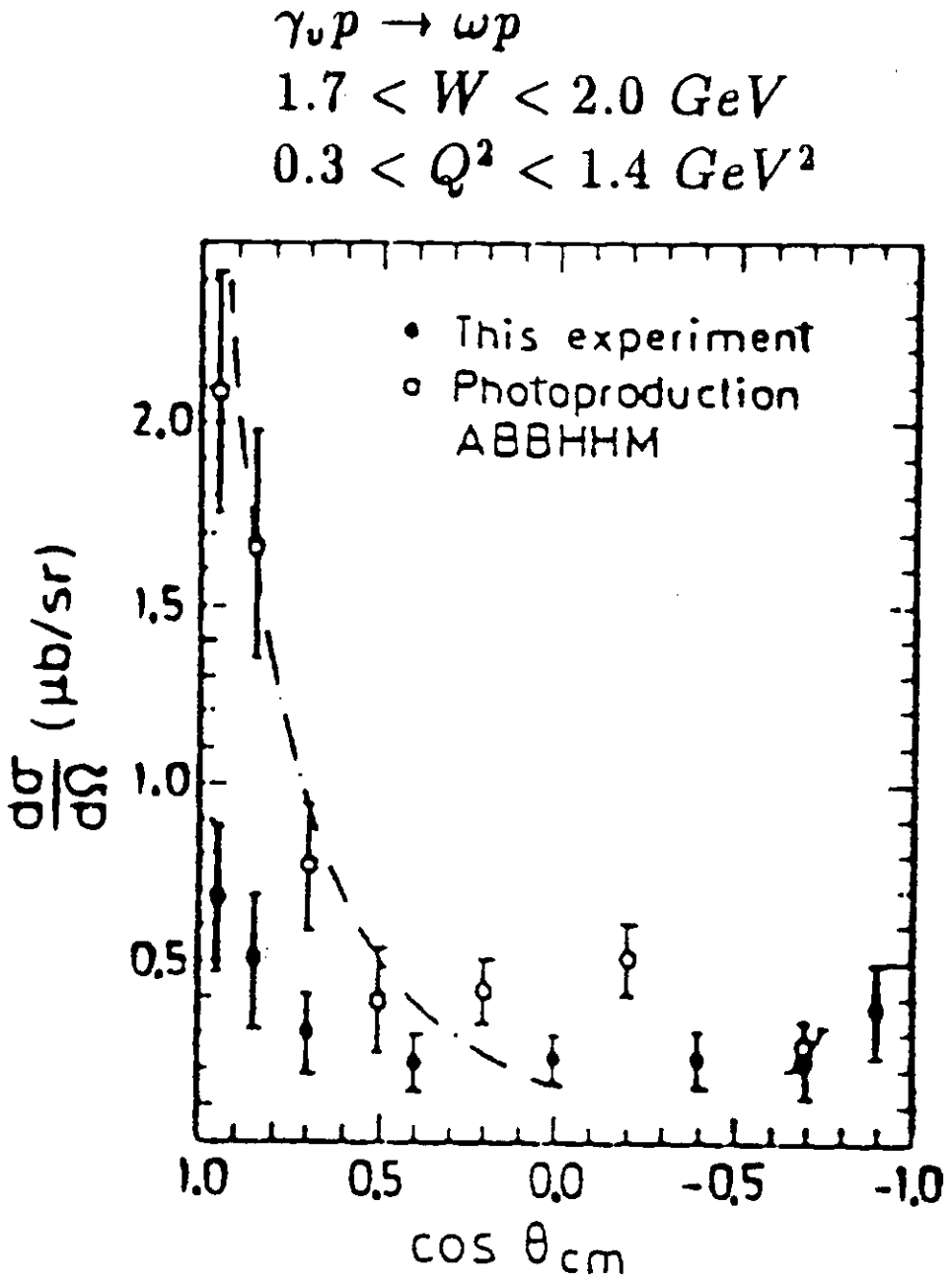
$\gamma_v p \rightarrow \omega p$
$1.7 < W < 2.0\ GeV$
$0.3 < Q^2 < 1.4\ GeV^2$
This experiment
Photoproduction
ABBHHM
$\frac{d\sigma}{d\Omega}$ (μb/sr)
2.0
1.5
1.0
0.5
1.0
0.5
0.0
-0.5
-1.0
cos θ cm

Fig.2

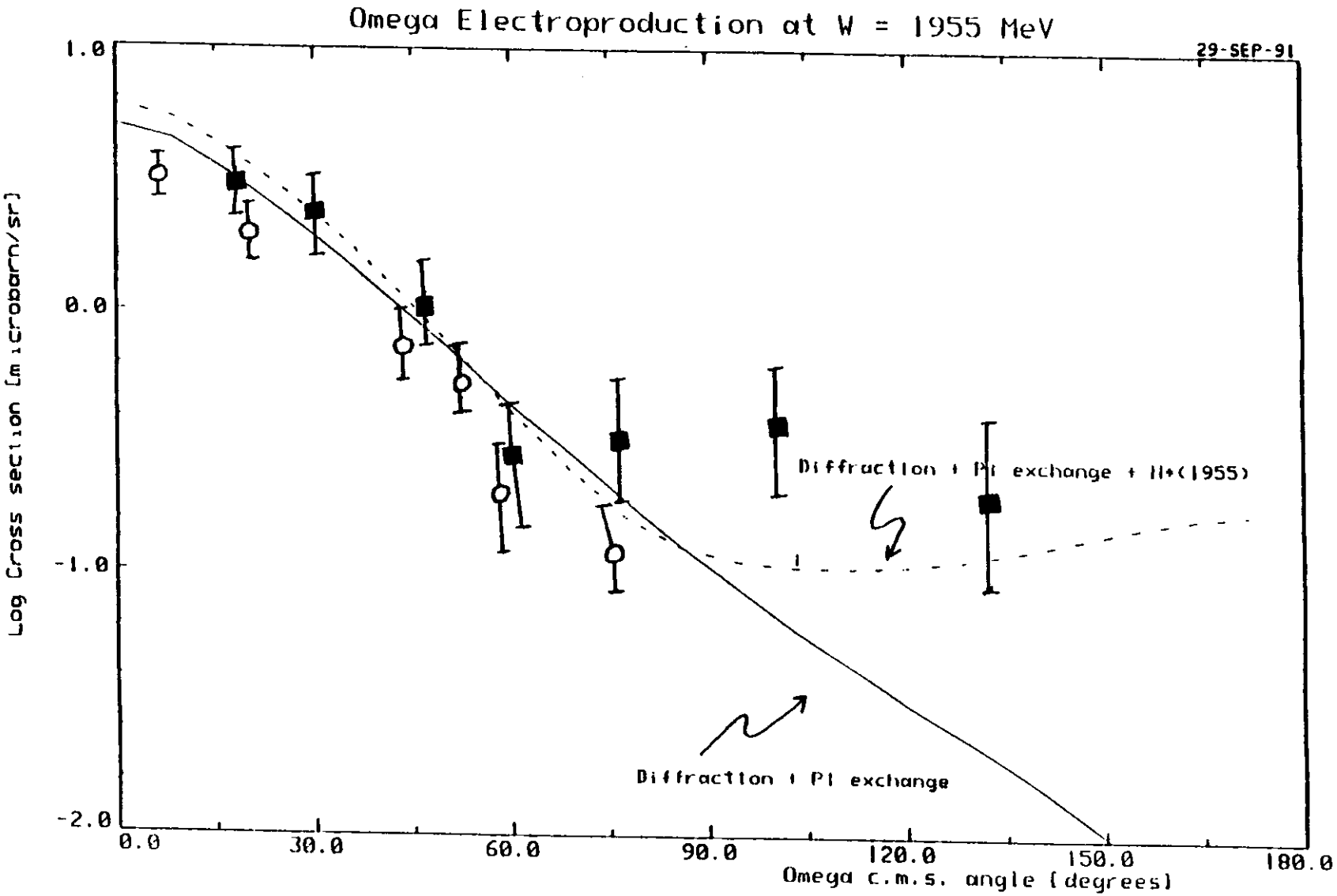
Omega Electroproduction at W = 1955 MeV
29-SEP-91
1.0
0.0
-1.0
-2.0
Log Cross section [microbarn/sr]
0.0
30.0
60.0
90.0
120.0
150.0
180.0
Omega c.m.s. angle (degrees)
Diffraction + Pi exchange + N*(1955)
Diffraction + Pi exchange

Fig.3

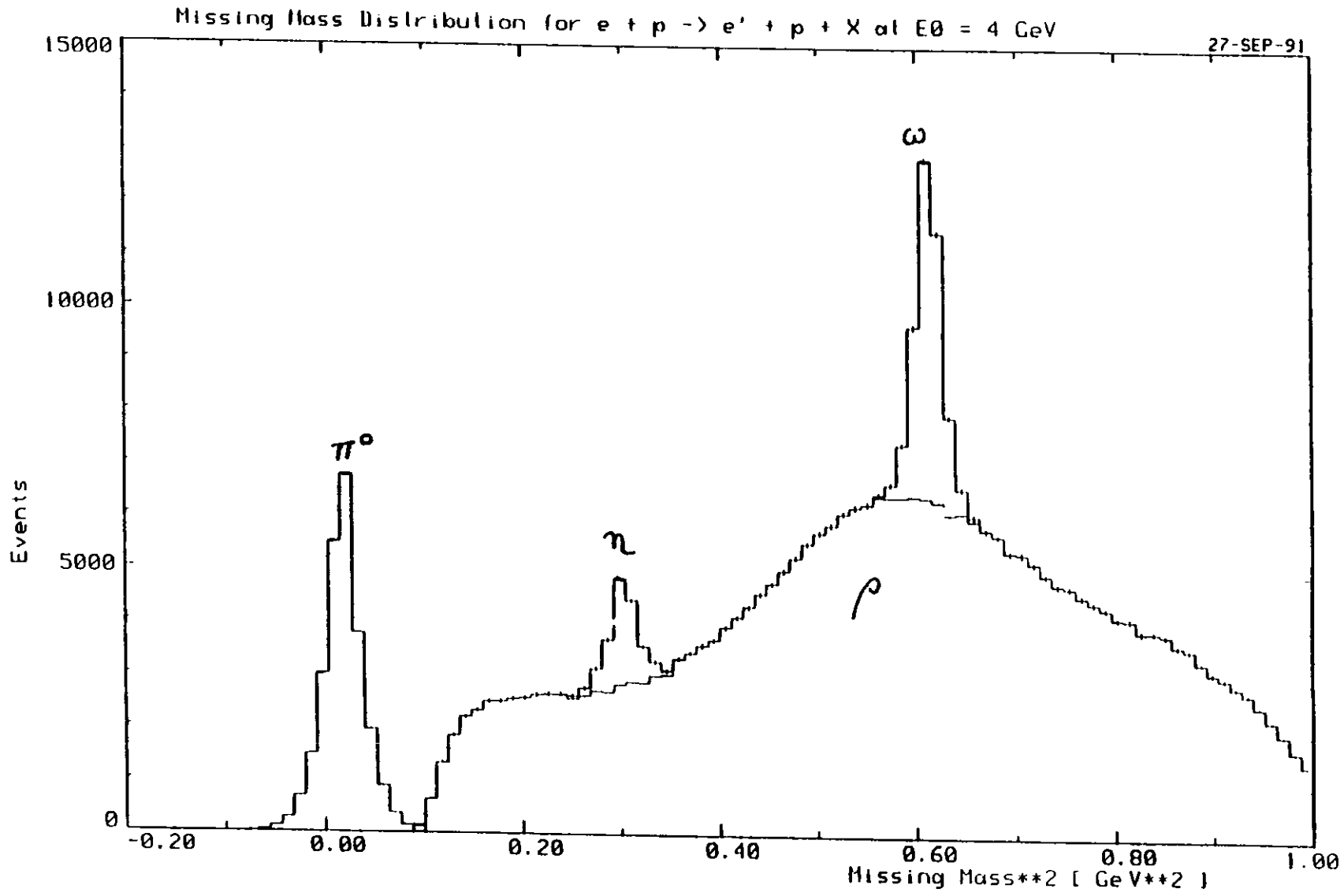
Missing Mass Distribution for e + p -> e' + p + X at E0 = 4 GeV
27-SEP-91
15000
10000
5000
0
Events
π°
η
ρ
ω
-0.20
0.00
0.20
0.40
0.60
0.80
1.00
Missing Mass**2 [GeV**2]

Fig.4

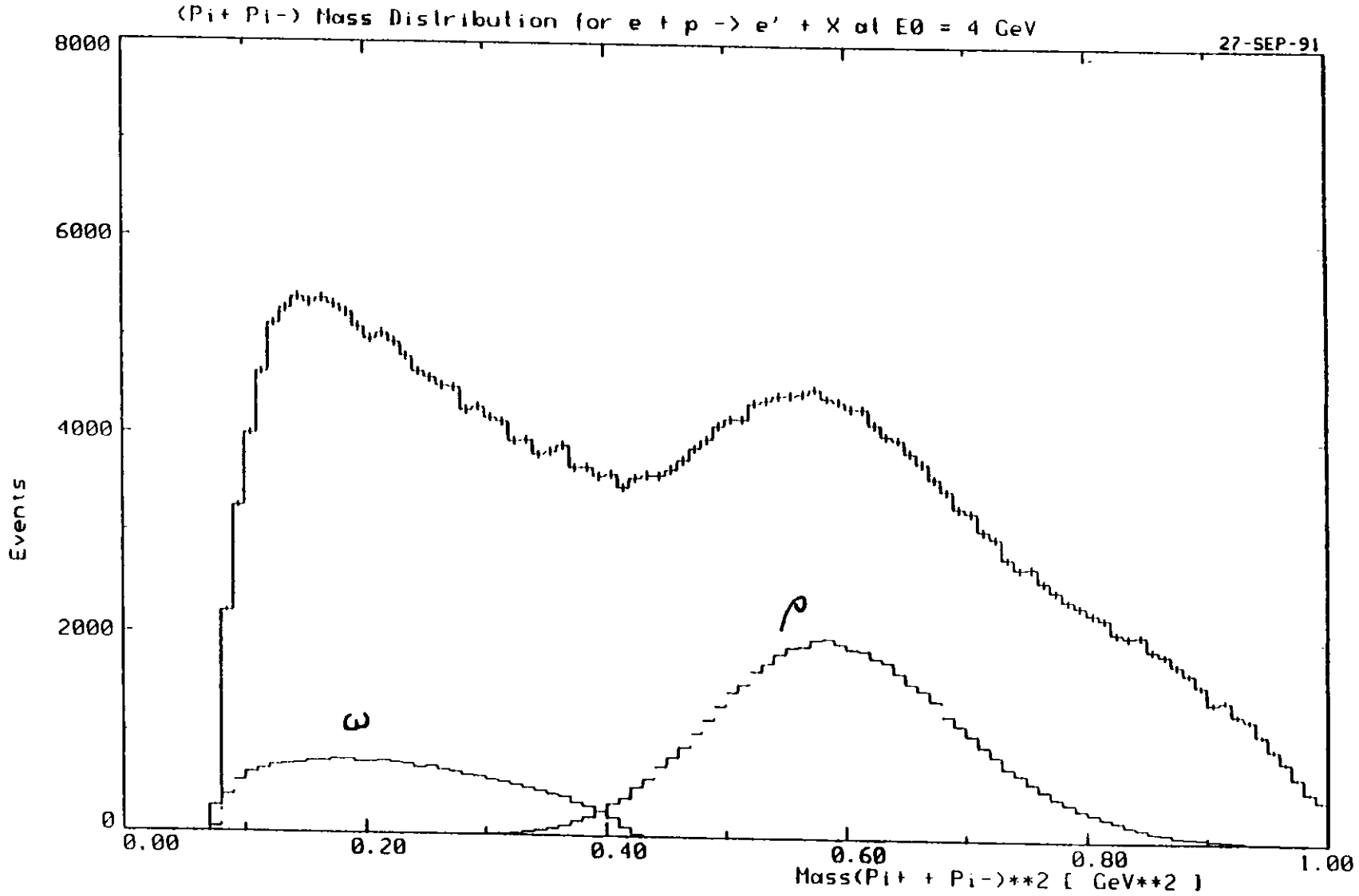
(Pi+ Pi-) Mass Distribution for e + p -> e' + X at E0 = 4 GeV
27-SEP-91
8000
6000
4000
2000
0
Events
ω
ρ
0.00
0.20
0.40
0.60
0.80
1.00
Mass(Pi+ + Pi-)**2 [GeV**2]

Fig.5

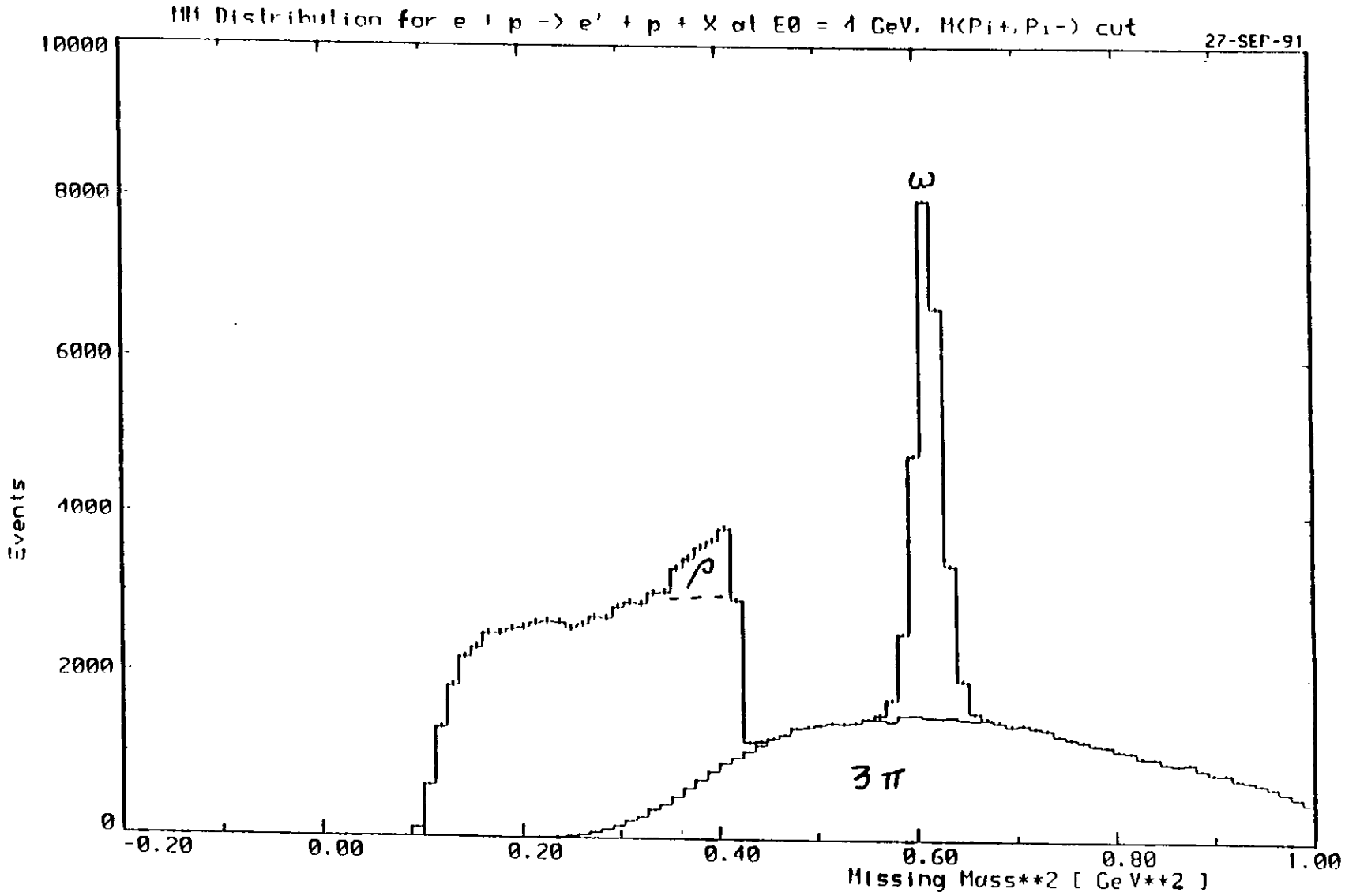
MM Distribution for e + p -> e' + p + X at E0 = 4 GeV, M(Pi+,Pi-) cut
27-SEP-91
10000
8000
6000
4000
2000
0
Events
ω
ρ
3π
-0.20
0.00
0.20
0.40
0.60
0.80
1.00
Missing Mass**2 [GeV**2]

Fig.6

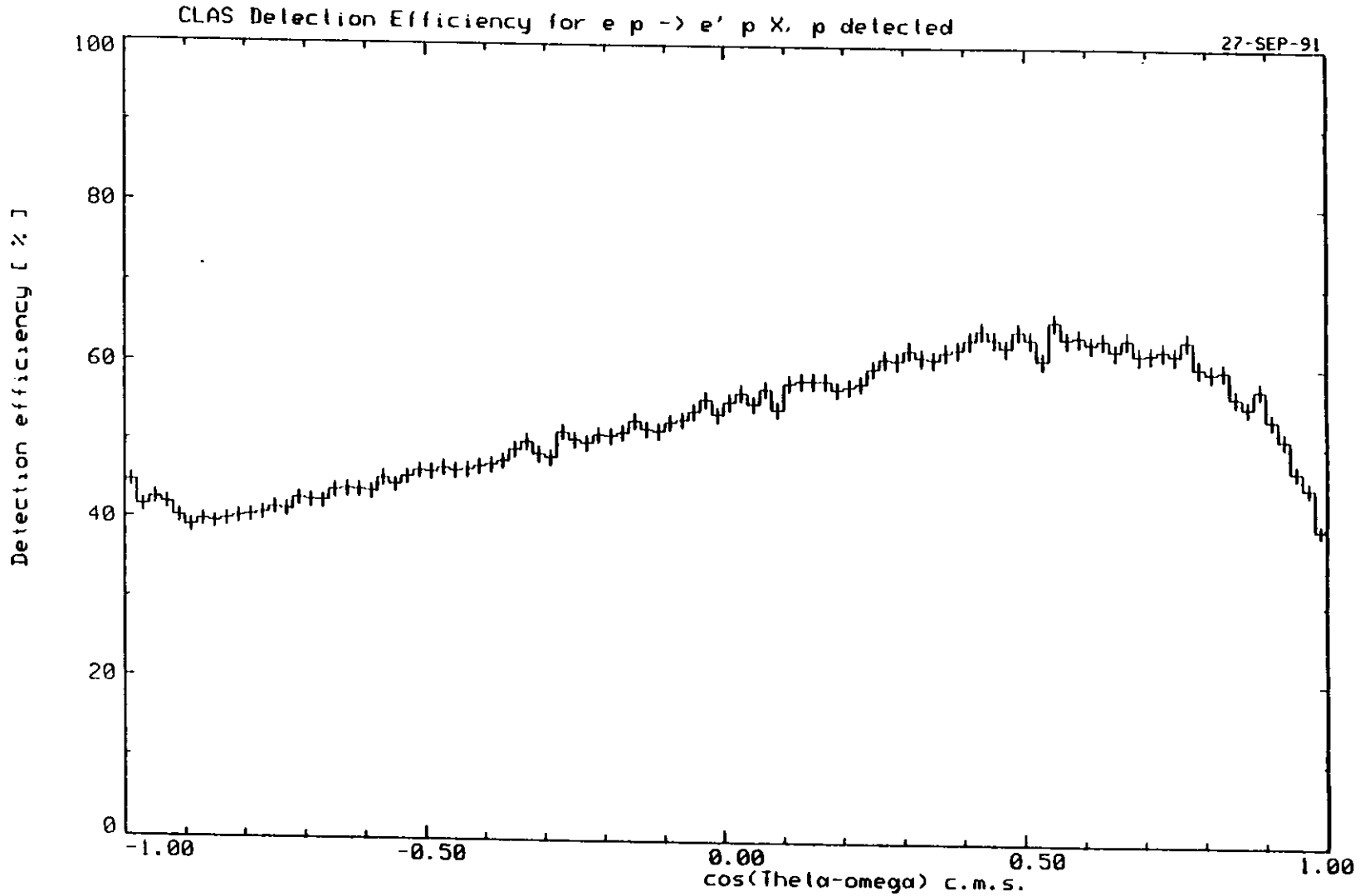
CLAS Detection Efficiency for e p -> e' p X, p detected
27-SEP-91
Detection efficiency [%]
100
80
60
40
20
0
-1.00
-0.50
0.00
0.50
1.00
cos(Theta-omega) c.m.s.

Fig.7

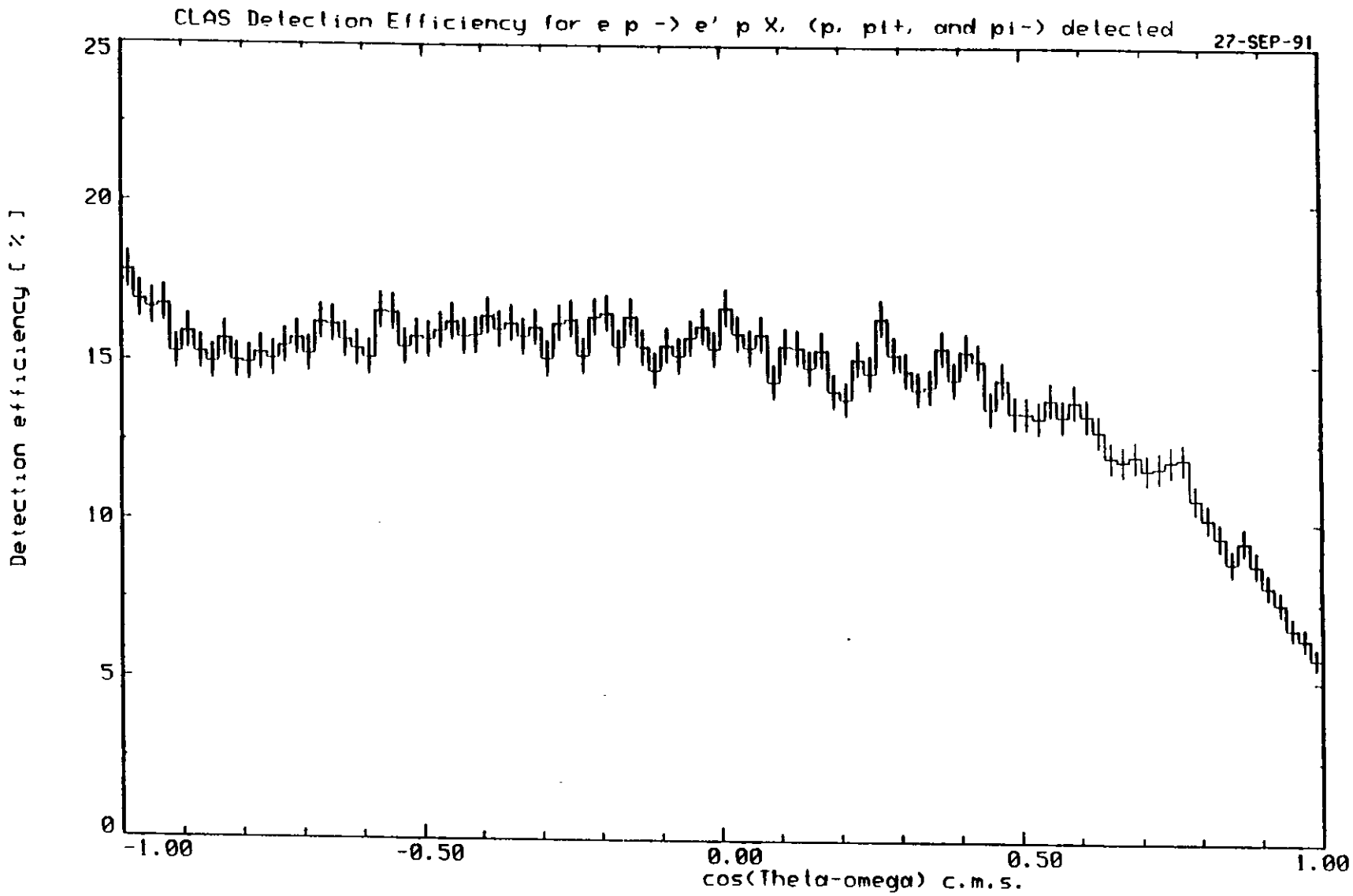
CLAS Detection Efficiency for e p -> e' p X, (p, pi+, and pi-) detected
27-SEP-91
Detection efficiency [%]
25
20
15
10
5
0
-1.00
-0.50
0.00
0.50
1.00
cos(Theta-omega) c.m.s.

Fig.8

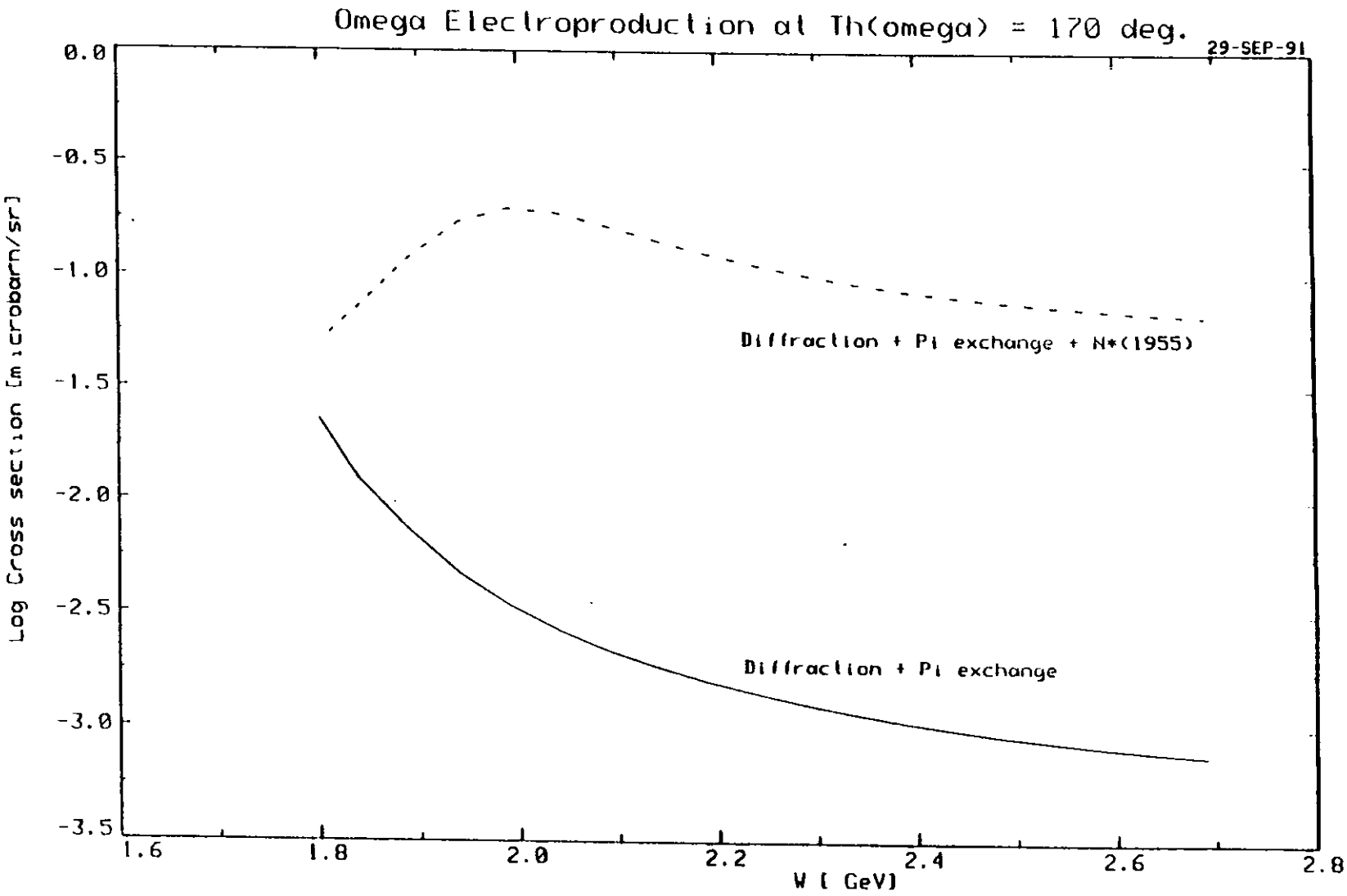
Omega Electroproduction at Th(omega) = 170 deg.
29-SEP-91
Log Cross section [microbarn/sr]
0.0
-0.5
-1.0
-1.5
-2.0
-2.5
-3.0
-3.5
1.6
1.8
2.0
2.2
2.4
2.6
2.8
W [GeV]
Diffraction + Pi exchange + N*(1955)
Diffraction + Pi exchange

Fig.9

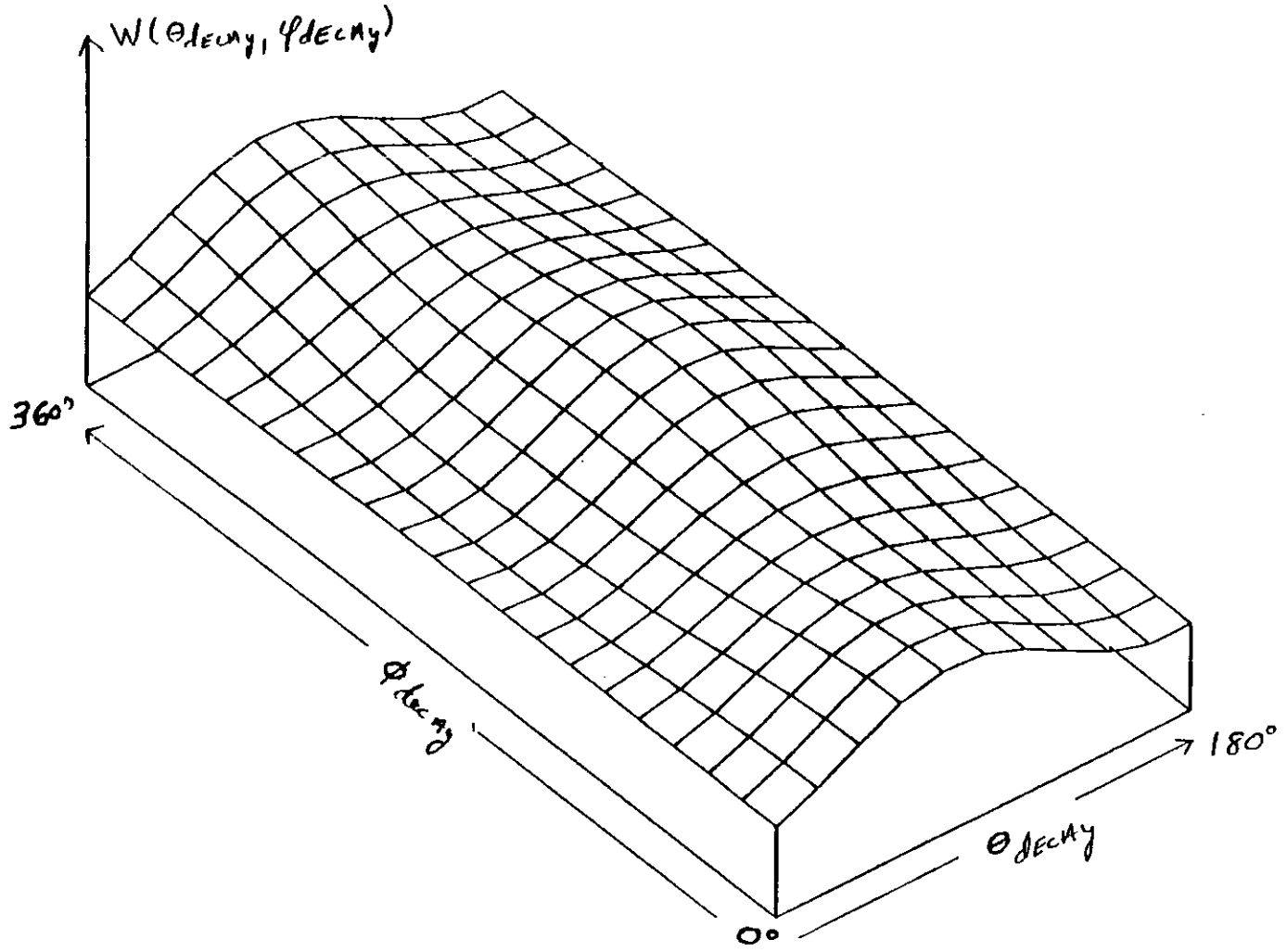

Fig.10

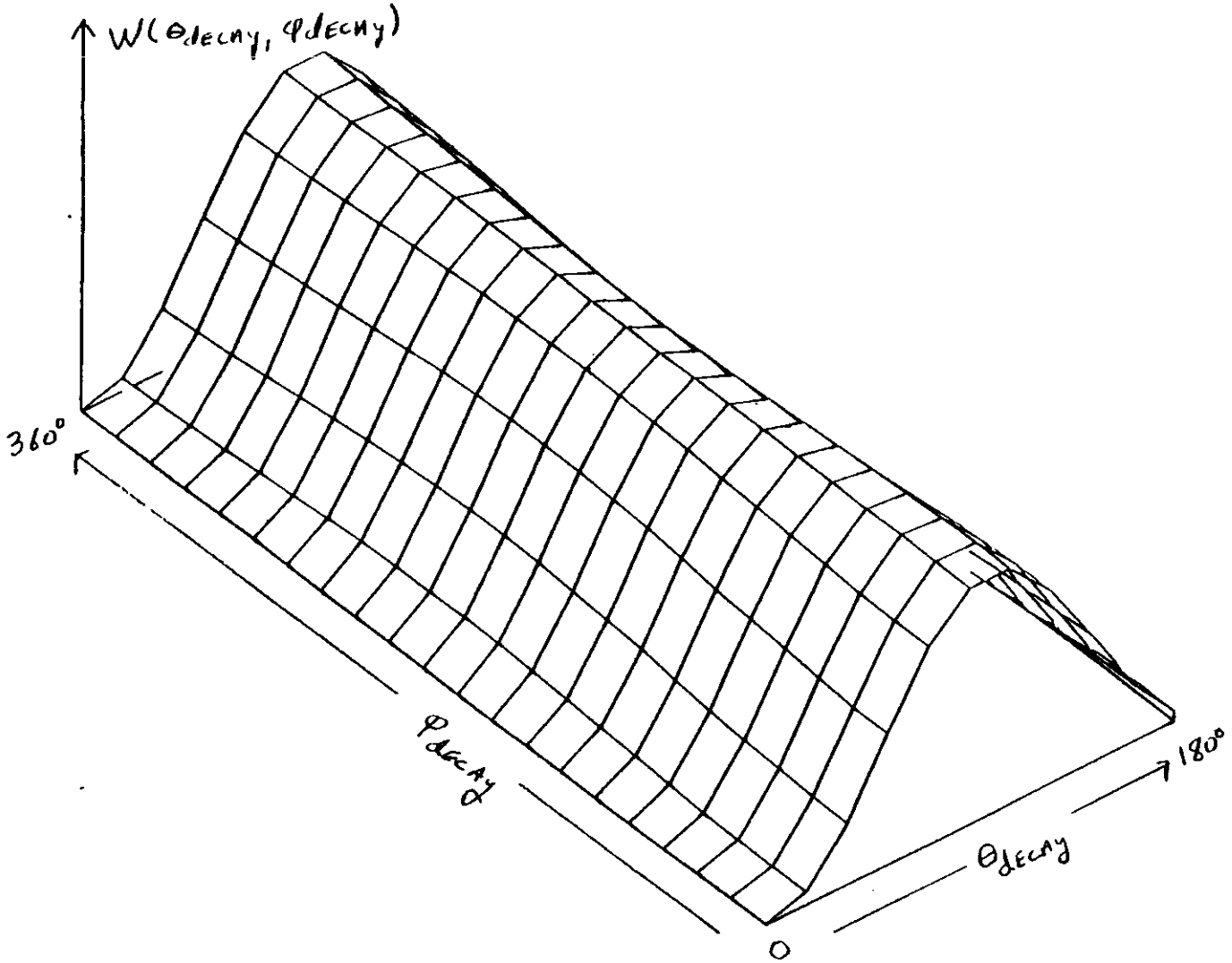

Fig.11